

# Monitoring of SF<sub>6</sub> Degradation in GIS Using Frequency Response Analysis

Mehdi Babaei and Ahmed Abu-Siada  
Curtin University, Perth, Western Australia

**Abstract**—Frequency Response Analysis (FRA) is generally used to detect any changes in the active part of the test object. Several studies have analyzed the effect of different mechanical changes including deformations and oil insulation decays on frequency response of transformers as a test object, however no research has ever studied the effect of gas degradation on frequency signature of a gas insulated substation (GIS). This paper investigates the possibility of using frequency response analysis to assess the quality of insulation medium in gas insulated substation (GIS). For this purpose, a single phase GIS filled with SF<sub>6</sub> between the main conductor and the enclosure is simulated in Maxwell 3D using finite element method to obtain the electrical parameters of the substation in real mode operation. Measurement of frequency response was carried out in GIS simulations with different insulation qualities from healthy to weak condition. The results show that the frequency response of GIS can disclose any minor deterioration in gas quality of the switchgear.

**Index Terms**—Gas Insulated Substation, SF<sub>6</sub>, Frequency Response Analysis, Insulation degradation

## I. INTRODUCTION

SULPHUR hexafluoride (SF<sub>6</sub>) is a non-toxic, inert, insulating and cooling gas of high dielectric strength and thermal stability which is used in gas insulated switchgears as insulation medium [1]. GIS insulation aging can reduce the dielectric strength of SF<sub>6</sub> due to frequent operation of disconnecting switches and circuit breakers [2, 3] which will result in some catastrophic failures if a reliable monitoring system is not applied to assess the quality of SF<sub>6</sub> regularly. Frequency response analysis (FRA) is one of the methods used in other high voltage applications such as power transformer to detect any mechanical faults and geometrical changes of internal components including coils and winding [4]. Some examples of conditions that FRA can be used to assess are damages following short-circuit or any faults during transportation, and following a seismic event.

The main concept used in FRA is that any mechanical changes in mechanical features of the test object results in some change in electrical parameters of the equivalent model of the object then results in some changes to the frequency response of the object. Existing methods to determine SF<sub>6</sub> degradation are based on measurements by several sensors connected to GIS, but hybrid systems compromising measurement and simulation methods have drawn considerable attention for the purpose of asset

management in electrical plants [5]. The detection of damage using FRA is most effective when frequency response measurement data is available from the object when it is in a known good condition which can be considered as a FRA signature of the object and can be used for assessing the condition of the object during its continuous operation [6]. Regarding the importance of gas insulation monitoring in GIS, this method can be applied in GIS to detect any probable dielectric deterioration in the substation which can FRA signature of GIS disclose.

To make a frequency response measurement, a low voltage signal is applied to one terminal of the test object with respect to the tank. The voltage measured at this input terminal is used as the reference signal and a second voltage signal (the response signal) is measured at a second terminal with reference to the tank. The frequency response amplitude is the scalar ratio between the response signal ( $V_{out}$ ) and the reference voltage ( $V_{in}$ ) (presented in dB) as a function of the frequency. The phase of the frequency response is the phase difference between  $V_{in}$  and  $V_{out}$  (presented in degrees). The measured FRA signature could be in the form of impedance instead of transfer function as well [7].

## II. SF<sub>6</sub> DEGRADATION

High dielectric strength of SF<sub>6</sub> is due to high electronegativity of fluorine, it means that the life span of the free electrons remains very low and with the SF<sub>6</sub> molecules they form heavy ions with low mobility. Then the probability of dielectric failure by a snowballing effect and electron removal from the gas under electrical field is delayed [8]. Also the thermal behavior of SF<sub>6</sub> is very stable due to the symmetrical shape of its molecules with one sulfur atom at the center and six fluorine atoms at the corners of the molecule. Following a breakdown, SF<sub>6</sub> regenerates itself. Its original strength is spontaneously restored and, in most cases, is even slightly enhanced. Due to the very low adiabatic coefficient of SF<sub>6</sub>, the pressure rise as a result of thermal expansion following dielectric breakdowns is less than that with other gases and very considerably less than is the case with liquid dielectrics [9]. These high quality features of SF<sub>6</sub> made it particularly suitable for application in power circuit breakers and high-voltage switchgears as well as in high voltage cables and transformers [8].

During the arcing time in SF<sub>6</sub> with very high temperature about 20,000°K, the gas breaks down and although SF<sub>6</sub> is chemically stable material, it decomposes into low number fluorine molecules such as SF<sub>2</sub> which are extremely toxic, corrosive materials. This created impurities can also deteriorate the insulating performance of SF<sub>6</sub> by reducing the dielectric strength of SF<sub>6</sub>[10]. Since gas insulated substations have been extensively used in power networks within recent few decades with SF<sub>6</sub> as insulating medium in an environment with large number of switching operation and frequent strikes due to their higher reliability and safety [2], special attention must be given to the condition monitoring of SF<sub>6</sub> in gas insulated substations.

Moisture ingress in GIS may have deteriorating effect on the insulation medium. Very high levels of humidity increase the possibility that water molecules will condense into the liquid phase, adversely affecting the dielectric withstand strength of GIS [11] and significantly increasing the possibility of flashover. Therefore, humidity in GIS should be maintained at a level such that the humidity does not condense in the form of liquid water over the entire range of the expected operating temperatures and gas pressures. Also the formation of corrosive and toxic decomposition by-products occurs in reactions between moisture and dissociated SF<sub>6</sub> found in the high energy arcs during normal switching operations. Higher concentrations of humidity can result in higher concentrations of decomposition by products [B3]. These by-products cause corrosion and may degrade insulators and other internal components within the GIS, and pose a safety hazard.

The dielectric property of insulation system is characterized based on two fundamental factors; permittivity and conductivity. While the permittivity affects insulation system behaviour during electrical transient conditions, electric conductivity plays an essential role to specify the dielectric strength of insulating system [12]. SF<sub>6</sub> degradation is usually accompanied with change in both insulation permittivity and conductivity which results in change in the capacitance between GIS main conductor and the enclosure. This change in capacitance value can be described by [13]:

$$\epsilon^* = \frac{\epsilon}{\epsilon_0} = \epsilon_r - j\epsilon'' = \epsilon_r - j\frac{\sigma}{\omega} = \frac{C(\omega)}{C_0} \quad (1)$$

where,  $\epsilon$ ,  $\epsilon^*$ ,  $\epsilon_0$  and  $\epsilon_r$  refer to the total, complex, vacuum and relative permeability, respectively.  $\sigma$  is the electrical conductivity (S.m<sup>-1</sup>) and  $\omega$  is the frequency (rad.s<sup>-1</sup>). Eq. (1) clarifies that GIS capacitance is significantly dependent on dielectric permittivity and conductivity. Any change in these factors will be reflected as a kind of change in capacitance. Table 1 shows the electrical characteristics of SF<sub>6</sub>.

TABLE 1. CHARACTERISTICS OF SF<sub>6</sub>

| Parameter               | Description     |
|-------------------------|-----------------|
| Dielectric breakdown    | 89 V/mPa        |
| Relative permittivity   | 1.00204         |
| Electrical conductivity | 1e-16 Siemens/m |

### III. GIS MODELLING USING FINITE ELEMENT METHOD

For the purpose of studying the effect of SF<sub>6</sub> aging or degradation on frequency response signature of GIS, SF<sub>6</sub> permittivity and conductivity are changed to particular levels. These minor changes in insulation characteristics of SF<sub>6</sub>, reflect as changes in the series capacitance of GIS conductor which can appear in changes in distributed parameter model of GIS. In this paper, the feasibility of utilizing FRA in recognizing SF<sub>6</sub> degradation is investigated through the simulation of a real 400kV gas insulated substation located in the north of Iran. The single line diagram and arrangement of equipment are obtained from [14, 15]. Arrangement of GIS equipment and gas compartments are shown in Fig.1. It is shown in Fig.1 that each transformer feeder is assembly of several high voltage equipment such as circuit breaker, disconnecting switch and instrument transformers connected in double busbar arrangement with bypass disconnecting switch. Each equipment is located in its own gas compartment enclosed by aluminum enclosure. The space between GIS conductor and the enclosure contains SF<sub>6</sub> as insulating medium.

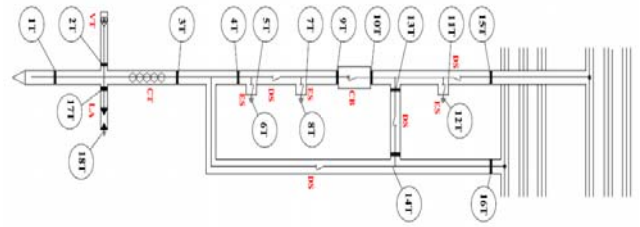


Fig. 1. Gas compartments of GIS equipment

According to Fig. 2, all GIS sections are modelled as distributed parameter line with R, L, and C parameters calculated by finite element method. It means that all GIS compartments are simulated in Maxwell 3D software in three dimensional real model as shown in Fig. 3 to Fig. 5 and the capacitance and inductance of each compartment are computed using electrostatic and magnetostatic solvers of the software respectively.

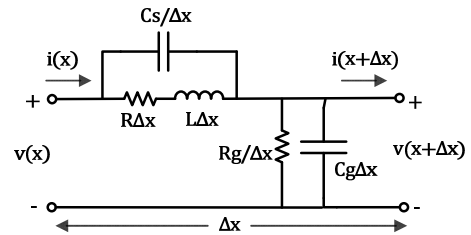


Fig. 2. Distributed parametr model of GIS sections

All solids modelled in the software are meshed by adaptive meshing operation and in order to obtain the set of algebraic equations to be solved, the geometry of the problem is discretized automatically into small elements which are called tetrahedral due to their shape and are produced by meshing operation. Capacitive elements are calculated by running the electrostatic solver of Maxwell 3D where voltage V is applied on GIS conductor, while

the voltage level is maintained at a level of zero on the aluminium enclosure. The energy stored in electrostatic field ( $W_{ij}$ ) between the two elements can be calculated as follows [16]:

$$W_{ij} = 0.5 \int_{Vol} D_i \times E_j dVol \quad (2)$$

Where  $W_{ij}$  is the electrical field energy between elements  $i$  and  $j$ ,  $D_i$  is the electrical flux density of element  $i$  and  $E_j$  is the electrical field intensity of element  $j$  and  $Vol$  is the volume of simulated object. The capacitance  $C_{ij}$  between two elements  $i$  and  $j$  can then be calculated as:

$$C_{ij} = 2 \times \frac{W_{ij}}{V^2} \quad (3)$$

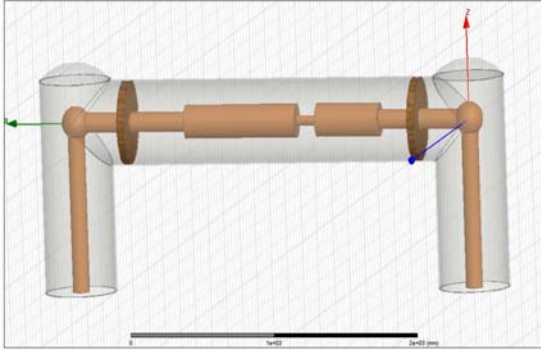


Fig. 3. Closed circuit breaker model in Maxwell 3d

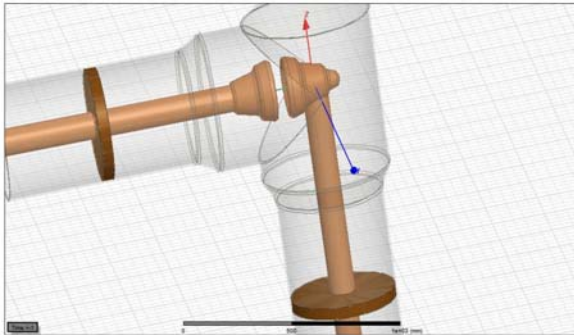


Fig. 4. Disconnecting switch model

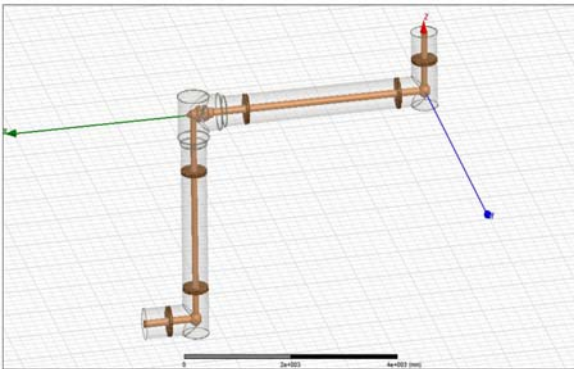


Fig. 5. 3D model of GIS connections

Inductive components are calculated based on the average of the magnetic field energy ( $W_{ij}$ ) and the

corresponding peak current passing through the conductor ( $I_p$ ) as follows[16]:

$$W_{ij} = 0.5 \int_{Vol} B \times H dVol \quad (4)$$

$$L_{ij} = 2 \times \frac{W_{ij}}{I^2} \quad (5)$$

where  $B$  is the magnetic field density,  $H$  is the magnetic field intensity, and  $Vol$  is the conductor volume. Resistive components are calculated based on power losses ( $P_{loss}$ ) depending on conductor conductivity ( $\sigma$ ) and current density ( $J$ ) as given in (5) and (6) below [12]:

$$P_{loss} = \left(\frac{1}{2\sigma}\right) \int_{Vol} J \cdot J dVol \quad (6)$$

$$R = P_{loss}/I^2 \quad (7)$$

Table 2 in lists the calculated GISequivalent circuit parameters.

TABLE 2. GIS PARAMETERS

| Parameter                        | Description |
|----------------------------------|-------------|
| External radius of GIS conductor | 60 mm       |
| Internal radius of GIS conductor | 42.5 mm     |
| External radius of enclosure     | 254 mm      |
| Internal radius of enclosure     | 246.1 mm    |

#### IV. IMPACT OF SF<sub>6</sub> DEGRADATION ON GIS FRA SIGNATURE

In this section, three different levels are defined for SF<sub>6</sub> degradation as presented in Table 3: slight, moderate and significant variation in gas dielectric characteristics based on 5%, 10% and 15% change in permittivity of SF<sub>6</sub> respectively. Then the impact of gas degradation on FRA signature of GIS is studied by applying frequency response analysis on GIS switchgear. FRA signature of GIS is presented in Fig. 6 by applying the FRA measurement on healthy insulation system and is considered as a base case for being compared with the frequency response of degraded SF<sub>6</sub>. The signature is obtained by sweeping an AC low voltage source and variable frequency (up to 10 MHz) on the terminal of SF<sub>6</sub>/Air bushing in line feeder or cable termination in transformer feeder and calculating the input current. The FRA signature is plotted in the form of GIS input impedance in dB. ( $Z_{in} = \log_{10}(V_{in}/I_{in})$ ) for varying frequency. Then the FRA of GIS is obtained by repeating the described procedure in each defined case of degradation level.

TABLE 3. SF<sub>6</sub> DEGRADATION LEVEL

| Level                 | Base | slight | moderate | Significant |
|-----------------------|------|--------|----------|-------------|
| Relative permittivity | 1    | 1.1    | 1.2      | 1.3         |

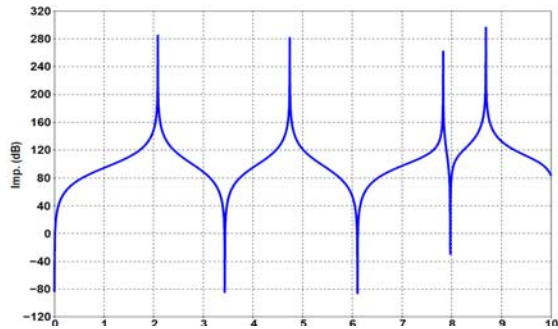


Fig. 6. FRA signature of GIS as base case

As shown in Fig. 6, there are several resonance and anti-resonance appearing in FRA signature of GIS and at higher frequencies the resonance frequencies are much less significant due to dominance of capacitive characteristics of GIS components in comparison with inductive characteristics of GIS conductor. Fig. 7 to Fig. 9 show the FRA of GIS in other health conditions of SF<sub>6</sub> and compares the FRA with the base case. The impact of SF<sub>6</sub> degradation is reflected as slight shift in FRA signature toward low frequencies with respect to the FRA of the base case and the severity of this shift is dependent on the severity of SF<sub>6</sub> degradation.

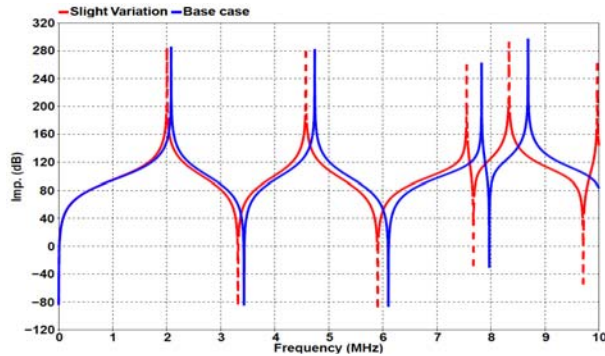


Fig. 7. Slight SF<sub>6</sub> degradation on FRA signature

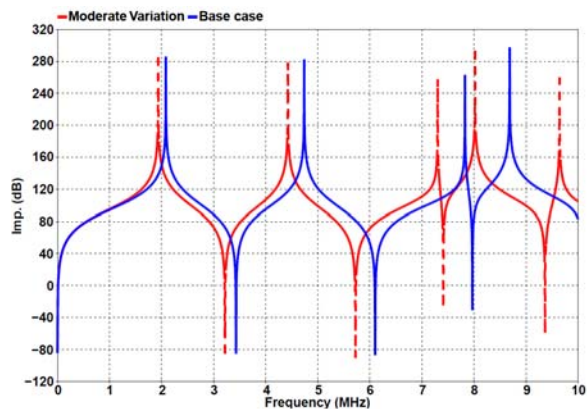


Fig. 8. Moderate SF<sub>6</sub> degradation on FRA signature

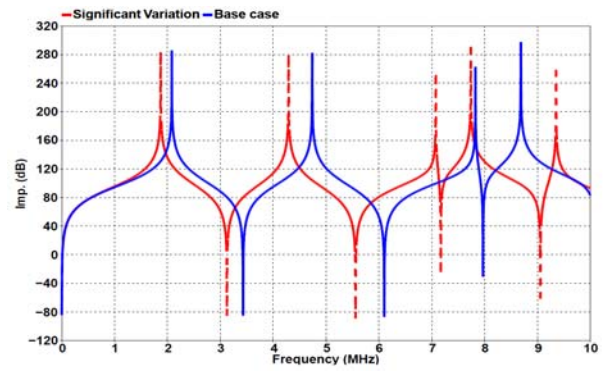


Fig. 9. Significant SF<sub>6</sub> degradation on FRA signature

The above results show that FRA has a potential to detect SF<sub>6</sub> aging / degradation. The effect of oil degradation is noticeable for frequency ranges above 1MHz where resonance frequencies tend to shift to the left. The impact is more pronounced with the increase of SF<sub>6</sub> degradation level.

## V. CONCLUSION

In this study, the concept of using the frequency response of an object for the purpose of detecting the changes in electrical characteristics of that object was applied to gas insulated substation to detect the amount of degradation level of SF<sub>6</sub>. Gas insulated substation was simulated in EMTP-RV by distributed parameter model of equipment. The parameter were calculated by modelling in three dimensional real geometry and running finite element analysis. Simulation results show that SF<sub>6</sub> aging / degradation introduces a reduction to the resonance and anti-resonance frequencies in the high frequency range. Also, the magnitude of the FRA signature is slightly decreased within the mid frequency range. Furthermore, this method has advantage over other existing methods of using gas system sensors on local control cabinets of GIS regarding the higher reliability of the proposed FRA signature method.

## REFERENCES

- [1] "IEEE Guide for Sulphur Hexafluoride (SF<sub>6</sub>) Gas Handling for High-Voltage (over 1000 Vac) Equipment," *IEEE Std C37.122.3-2011*, pp. 1-69, 2012.
- [2] Maziar Babaei, Mehdi Babaei, and G. Nourirad, "Analysis of Influential Factors in Determining Very Fast Transient Overvoltages of GIS Substations," presented at the 2014 IEEE 8th International Power Engineering and Optimization Conference (PEOCO2014), Langkawi/Malaysia, 2014.
- [3] Mehdi Babaei, Ahmed Abu-Siada, and Maziar Babaei, "Suppressing resonance in transformer winding under very fast transient overvoltage," in *2016 IEEE Innovative Smart Grid Technologies - Asia (ISGT-Asia)*, 2016, pp. 1037-1042.
- [4] A. Abu-Siada, N. Hashemnia, S. Islam, and M. A. S. Masoum, "Understanding power transformer frequency response analysis signatures," *IEEE Electrical Insulation Magazine*, vol. 29, pp. 48-56, 2013.
- [5] Maziar Babaei, Jian Shi, Nasibeh Zohrabi, and Sherif Abdelwahed, "Development of a hybrid model for shipboard power systems," in *2015 IEEE Electric Ship Technologies Symposium (ESTS)*, 2015, pp. 145-149.
- [6] O. M. Aljohani and A. Abu-siada, "Impact of power transformer insulating mineral oil degradation on FRA polar plot," in *2015 IEEE 24th International Symposium on Industrial Electronics (ISIE)*, 2015, pp. 567-572.
- [7] J. R. Secue and E. Mombello, "Sweep frequency response analysis (SFRA) for the assessment of winding displacements and deformation in power transformers," *Electric Power Systems Research*, vol. 78, pp. 1119-1128, 6// 2008.
- [8] R. J. V. Brunt and J. T. Herron, "Fundamental processes of SF<sub>6</sub> decomposition and oxidation in glow and corona discharges," *IEEE Transactions on Electrical Insulation*, vol. 25, pp. 75-94, 1990.
- [9] S. Theoleyre, "Cahier technique n° 193: MV breaking techniques " in *Collection Technique*, G. Schneider, Ed., ed, 1999.
- [10] F. Y. Chu, "SF<sub>6</sub> Decomposition in Gas-Insulated Equipment," *IEEE Transactions on Electrical Insulation*, vol. EI-21, pp. 693-725, 1986.
- [11] T. Nitta, Y. Shibuya, Y. Fujiwara, Y. Arahata, H. Takahashi, and H. Kuwahara, "Factors Controlling Surface Flashover in SF<sub>6</sub> Gas Insulated Systems," *IEEE Transactions on Power Apparatus and Systems*, vol. PAS-97, pp. 959-968, 1978.
- [12] O. Aljohani, A. Abu-siada, and S. Islam, "Impact of insulating oil degradation on the power transformer frequency response analysis," in *2015 IEEE 11th International Conference on the Properties and Applications of Dielectric Materials (ICPADM)*, 2015, pp. 396-399.
- [13] E. J. Murphy and S. O. Morgan, "The dielectric properties of insulating materials, III alternating and direct current conductivity," *The Bell System Technical Journal*, vol. 18, pp. 502-537, 1939.
- [14] Mehdi Babaei, Maziar Babaei, and M. Niasati, "Parametric Analysis of Over-voltages Caused by Back-flashover In Siah-bishe 400kV GIS Substation," presented at the 3rd International Conference on Electric Power and Energy Conversion Systems (EPECS 2013), Yildiz Technical University, Istanbul, Turkey, 2013.
- [15] Maziar Babaei, Sherif Abdelwahed, and Mehdi Babaei, "Transient Ground Potential Rise in Gas Insulated Substations and analysis of Effective Factors," presented at the ASME 2015 Power Conference collocated with the ASME 2015 9th International Conference on Energy Sustainability, the ASME 2015 13th International Conference on Fuel Cell Science, Engineering and Technology, and the ASME 2015 Nuclear Forum, 2015.
- [16] "Ansoft Maxwell," vol. REV 6.0, ed. Canonsburg: ANSYS Inc, 2012.